Preparation of Fischer–Tropsch Catalysts

P. A. Chernavskii

Department of Chemistry, Moscow State University, Moscow, 117234 Russia

Received September 24, 2004

Abstract—Topochemical processes accompanying the preparation of supported cobalt catalysts for Fischer–Tropsch synthesis are systematized. The influence of different factors on the size distribution of Co particles during catalyst preparation is considered. Using a magnetic method, it is possible to estimate the average particle size of the supported metal and to obtain a particle size distribution function. Approaches allowing one to control the type of size distribution function for the Co particles are described using Co/SiO$_2$ catalysts as an example.

Fischer–Tropsch synthesis is a catalytic process with a 75-year history. In recent years, this process has regained researchers' interest for several reasons. First of all, it is a method for "pure" fuel production. Furthermore, it is economically reasonable to convert gaseous hydrocarbons into a liquid fuel because of the large sources of natural gas deposited in remote districts. Cobalt-based catalysts for Fischer–Tropsch synthesis are especially interesting from the commercial point of view due to their rather high activity and selectivity with respect to linear hydrocarbons and their low cost as compared to the cost of catalysts based on noble metals.

The active phase (metallic Co) is usually deposited on an inert support with a developed surface. Many patents concerning the preparation of Fischer–Tropsch catalysts indicate that the approach to this problem is empirical, because the complicated topochemical processes that accompany the synthesis of the catalysts are poorly understood. In addition, the dependence of the selectivity of Fischer–Tropsch catalysts on the Co particle size remains unclear. The selectivity of the process is believed [1] to be independent of the Co particle diameter. At the same time, several authors believe that the highest selectivity toward hydrocarbons with more than 5 carbon atoms (C_5^+) is achieved at an optimum size of Co particles [2]. It is most likely that the nature of the support is also significant and has an effect on the selectivity [3]. According to [4], this effect is determined by the interaction between Co and the support. However, all the above-listed aspects are intimately interrelated, and, most likely, none of the factors determining the selectivity and activity of cobalt-based Fischer–Tropsch catalysts can be pointed out.

In the general case, the reducibility and particle size of the metal phase depend on the support nature [5], preparation method [6], metal content [7], and temperature regimes at the catalyst preparation stages [8].

The influence of the support surface is mainly determined by two factors: (1) the degree of chemical inertness toward the precursor, cobalt oxides, and metallic Co and (2) the pore structure of the support (specific surface area, pore volume, and pore diameter). As for the precursor, cobalt nitrate hexahydrate is the most popular compound used for this purpose. With organic acid salts as precursors, cobalt is more difficult to reduce to metal [9]. Such factors as the temperature regimes of preliminary drying, calcination, and reduction remain the most difficult to understand [10].

In this report, we focus on the drying, calcination, and reduction stages. Cobalt nitrate hexahydrate, Co(NO$_3$)$_2$ · 6H$_2$O, is used as the precursor, and silica gels with different pore structures serve as supports. The interrelation of factors determining the degree of reduction and particle size of metallic cobalt in the supported catalysts is illustrated in Fig. 1. The chemical nature of the support and precursor determines the type and degree of active component–support interaction. The granule size and pore structure of the support determine the diffusion component of the topochemical pro-
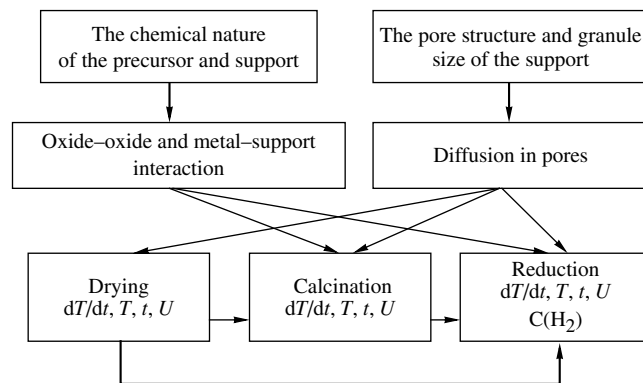
Fig. 1. Interrelation of different factors determining the extent of reduction and particle size of Co particles in supported cobalt catalysts.

cesses that yields the active phase (Co particles). Each of the consecutive stages of catalyst preparation (drying, calcination, and reduction) is affected by chemical or diffusion factors, as is shown by arrows in Fig. 1. We assume that no chemical reaction but the partial dehydration of $Co(NO_3)_2 \cdot 6H_2O$ occurs during drying. However, the granule size of the support, the specific surface area of the support, and the pore radius undoubtedly affect the drying rate. Several topochemical processes occur during calcination: the removal of water of crystallization, the formation and decomposition of hydroxo complexes, and the decomposition of the nitrate followed by oxide phase formation. The oxide phase can react with the support to form cobalt silicates in the case of silica gel. Diffusion plays an important role in these topochemical processes, determining the rate of the removal of gaseous products from the reaction zone. Reduction includes the chain of transformations $Co_3O_4 \longrightarrow CoO \longrightarrow Co$ and, perhaps, the reaction between CoO and SiO_2 yielding cobalt silicate. The diffusion component of the process affects the rate of water removal from the reaction zone and can determine the course of the overall process for supports with narrow pores.

Each of the stages considered is determined by a set of parameters, such as the rate of heating to the preset temperature (dT/dt), process temperature (T), the duration of isothermal heating (t), the flow rate of the gas phase (U), and the gas phase composition. The interplay of these parameters results in some set of Co nanoparticles, which is characterized by some frequency function of particle size $f(d)$ or weight $f(m)$. Hereafter, this function will be called distribution for simplicity. Note that most works dealing with this problem consider the relation between the preparation conditions and some average characteristics, such as the average particle size. This approach is not always correct. For instance, for the bimodal distribution, the average size may be physically meaningless because of the absence of particles of this size. Below, we show that a bimodal distribution can be observed for nearly all supports with a developed surface.

Transmission electron microscopy is generally used to study the size distribution of metal particles in supported catalysts. However, this method is very laborious, because many microphotographs should be processed to obtain a representative sample for deriving the desired distribution or a simple histogram. Chemisorption methods and the analysis of peak broadening in X-ray diffraction patterns can provide only average particle size data.

In several cases (see below), magnetic measurements may be of use in the characterization of the system of Co nanoparticles.
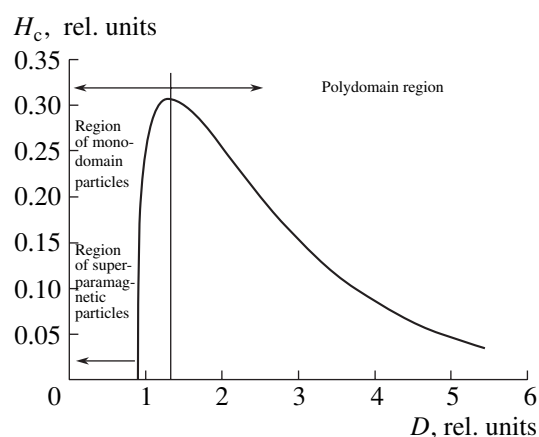

Fig. 2. Qualitative dependence of the coercive force (H_c) on the diameter of Co particles.

Magnetic Method for Determining the Cobalt Particle Size

The magnetic method of the determination of the particle size of ferromagnetic metals is based on the relation between the magnetization and the strength of the external magnetic field [11]. In the general case, this relation is a hysteresis loop characterized by at least three important parameters: σ_s (saturation magnetization), σ_r (residual magnetization), and H_c (coercive force). For Co particles with a diameter below 10 nm, which are superparamagnetic at room temperature, the hysteresis loop is degenerated into a sigmoid curve for which σ_r and H_c are zero. The residual magnetization and coercive force depend on the metal particle size. The analytical form of this function remains unknown. However, numerous experimental data [12] show that H_c as a function of Co particle diameter has a maximum at about 20 nm. A typical plot of H_c versus particle diameter is shown in Fig. 2. Particles with essentially different diameters ($d < 20$ nm and $d > 20$ nm) can correspond to the same H_c value (Fig. 2). This problem can be solved by a controlled oxidation of the metal particles. Low-temperature oxidation ($T < 300°C$) is known to produce an oxide film on metal particle surfaces. The thickness of this film varies only slightly with time and is temperature-dependent. Owing to the oxide film formation, the size of the metallic core of the particle decreases and, correspondingly, H_c changes. If the particle size exceeds 20 nm, H_c increases; if $d < 20$ nm, the coercive force decreases. It should be mentioned that H_c depends on the size of the largest particles in the system and, therefore, reflects the maximum size instead of the average size. We used this method for the first time to estimate the maximum size of the Co particles in the supported catalysts.

For a system containing no particles with $d > 20$ nm, the difference $1 - 2\sigma_r/\sigma_s$ is equal to the fraction of superparamagnetic particles, that is, the particles whose size is ≤10 nm [13]. Furthermore, a size distribution

Oxidation rate, rel. units
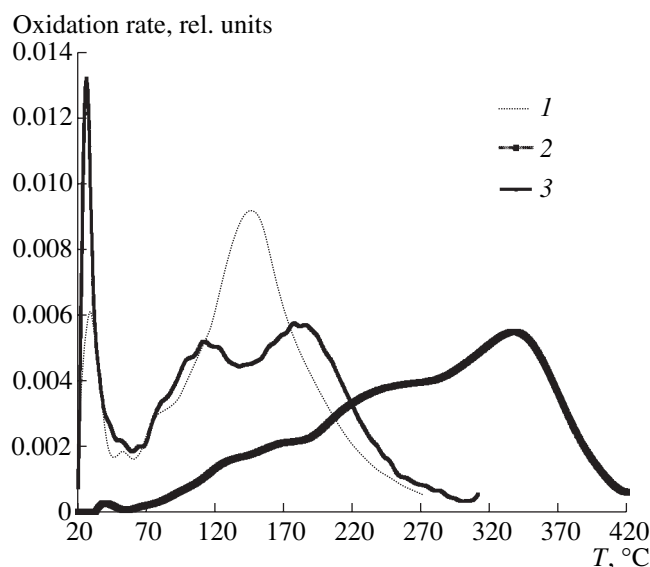
Fig. 3. Oxidation rate as a function of temperature for supported cobalt catalysts with an average Co particle size of (*1*) 6, (*2*) 8, and (*3*) 15 nm.

function can be obtained for this particle ensemble [14]. Our method for estimating the Co particle size in supported catalysts is advantageous to the other methods, because the measurements can be conducted *in situ* directly during catalyst preparation. This enables one to study different factors in both the particle size and the shape of the distribution function.

The temperature-programmed oxidation (TPO) method in combination with continuous magnetization measurements turned out to be very informative [15]. In this technique, the oxidation rate is derived from the rate at which magnetization decreases. Therefore, this technique reflects only the decrease in the amount of metallic cobalt, unlike the conventional TPO method, which provides oxygen absorption rate data.

According to the data presented in [16], the temperature at which the oxidation rate peak occurs in the TPO spectrum depends on the Co particle size: the smaller the particles, the lower this temperature. Furthermore, when the TPO spectrum contains two rate maxima, the particle size distribution is bimodal [16]. The oxidation rate as a function of temperature for a series of the Co/support catalysts with different average particle sizes is shown in Fig. 3. The first peak of the oxidation rate is observed for all of the systems studied and is due to the oxidation of the Co particles at room temperature at the moment of replacement of the inert gas flow with an oxygen-containing mixture. The greater the number of small particles in the system, the higher the initial oxidation rate. At room temperature, an oxide film with the thickness $\delta \approx 1$ nm is formed on the Co particles with a diameter of 6 nm, while the particles smaller than 2 nm are oxidized completely [17]. Under the assumption that the Co particles are spherical, one can

show [18] that δ is related to the particle radius as follows:

$$\delta = r\left[1 - \left(\frac{\sigma(t)}{\sigma_0}\right)^{1/3}\right], \qquad (1)$$

where σ_0 and $\sigma(t)$ are the magnetizations of the sample before and after oxidation for time t and r is the particle radius. Equation (1) makes it possible to estimate the average size of the Co particles if the magnetizations of the sample before and after oxidation at room temperature in air are known and δ is about 1 nm and does not depend considerably on the particle size.

Reduction Kinetics of Cobalt Oxides in Co/Support Systems

When considering topochemical processes in nanoparticles such as supported cobalt oxides one has to take into account the thermodynamic features of these systems. Nanoparticles have excess free energy as compared to bulky materials. This excess energy shifts phase equilibria in nanoparticles [19].

The equilibrium constant for a heterogeneous reaction involving nanoparticles depends on the particle size, because the chemical potential is size-dependent.
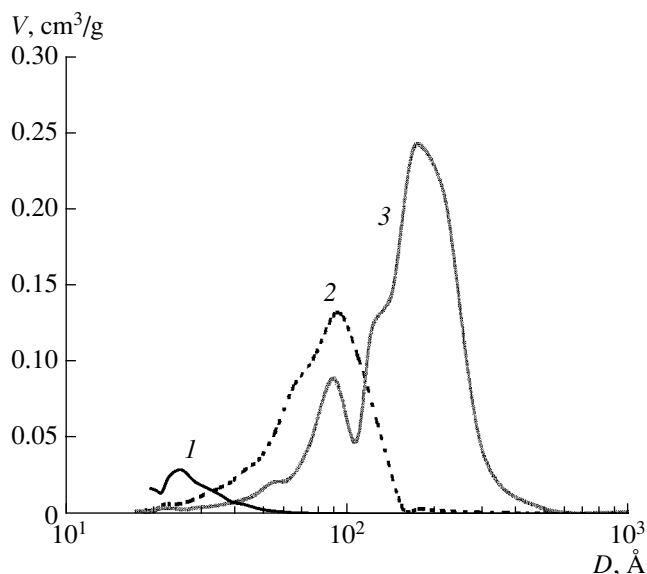
Numerous examples of the influence of the particle size on the equilibrium properties of the system have been reported [12, 20]. For this reason, we will discuss only one aspect of the thermodynamics of nanoparticles, namely, reactivity as a function of particle size, which is significant for further analysis.

It is well known that chemical equilibria are particle size dependent:

$$-\Delta G_d^\circ = RT\ln(K_d/K), \qquad (2)$$

where ΔG_d° is the change in the Gibbs energy related to the change in the particle size, K_d is the equilibrium constant of the reaction involving dispersed reactants, and K is the equilibrium constant for nondisperse reactants. A decrease in the particle size causes an enhancement of the activity of the reactants, and, accordingly, the equilibrium constant changes in some way, depending on the particle size of the starting substances and reaction products.

It can be shown that the equilibrium composition of the oxide system examined depends on both the curvature of the interfaces and the corresponding surface energies [21]. In the reduction of cobalt oxide nanoparticles, the partial hydrogen pressure should exceed the equilibrium pressure characteristic of the massive phase. In other words, for each partial hydrogen pressure, there is a critical particle size such that smaller oxide particles cannot be reduced. Similar results are reported in [22]. We obtained an experimental proof for the above thermodynamic deductions [21]. In particular, the parameters of particle size distribution depend on the partial hydrogen pressure during reduction. This
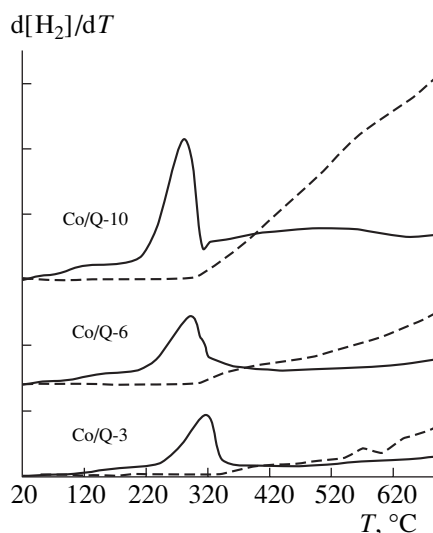
Fig. 4. Pore size distribution functions (V) for the silica gels (*1*) Q-3, (*2*) Q-6, and (*3*) Q-10.

Fig. 5. TPR spectra (solid lines) and magnetization curves recorded during TPR (dashed lines) for catalysts with a granule size of 0.1 mm.

fact suggests another interpretation for the results of the temperature-programmed reduction (TPR) studies. A comparatively low partial hydrogen pressure (~5% H_2 in Ar, ~37 Torr) is generally used in the TPR method. We have shown that the TPR spectrum of the catalyst depends on the size distribution of Co particles [15]. The data obtained in the present work show that the opposite is also true: the size distribution of metal particles depends on the partial hydrogen pressure used in the TPR experiment. Undoubtedly, this should be taken into account in TPR studies of supported metal catalysts.

Reduction kinetics depend on the oxide particle size, partial hydrogen pressure, and the pore structure of the support, because reduction can be controlled by kinetics or external or internal diffusion, depending on the size of the support pores.

To study the influence of diffusion factors on the reduction of cobalt oxides, we used a support with a known pore diameter distribution.

The catalysts to be studied were prepared by impregnating a support with a solution of cobalt nitrate of known concentration. The supports were CARIACT silica gels (Fujisilysia Chemical Ltd.; Q-3, Q-6, and Q-10 brands) with a narrow pore size distribution. The pore size distribution and the specific surface area of the silica gels were determined by low-temperature nitrogen adsorption. The experimental pore size distribution functions are presented in Fig. 4. The average pore size in the supports Q-3, Q-6, and Q-10 is 3, 6, and 10 nm, respectively; the specific surface is 550, 450, and 300 m^2/g, respectively. The silica gel Q-10 has a bimodal pore distribution function peaking at 9 and 11 nm.

The comparative TPR spectra for the catalysts Co/Q-3, Co/Q-6, and Co/Q-10 with a granule size of 0.1 mm are presented in Fig. 5 along with the corresponding magnetization curves recorded during TPR. The data in Fig. 5 show that, as the specific surface area increases or the pore size decreases, the reduction rate decreases and the maximum temperature of the main peak increases from 290°C for Co/Q-10 to 320°C for Co/Q-3. The amount of hydrogen required for the reduction of Co_3O_4 to CoO decreases by a factor of 2 on going from Co/Q-10 to Co/Q-3. It can be assumed that part of the Co_3O_4 interacts with silanol groups of the silica gel during reduction to yield a surface silicate, which is reduced only at elevated temperatures [10].

Continuous magnetization measurements provide information concerning only one step of the isothermal reduction of supported Co_3O_4, specifically, the transformation of CoO into Co. This allows one to avoid some of the difficulties encountered in the interpretation of data obtained by other methods (e.g., those arising from the processes $Co_3O_4 \longrightarrow CoO$ and $CoO \longrightarrow Co$ occurring in parallel).

An analysis of the reduction kinetics of the same catalyst at different temperatures shows that the conversion-vs.-time plots cannot always be transformed into one curve of this family by an affine transformation (by changing the time scale). Kinetic curves will be affine if the rate-determining steps pertain to one reaction zone [23]. The isothermal reduction experiment shows that the affinity of the conversion-vs.-time curves depends on the pore diameter. For instance, for a support with an average pore diameter of 10 nm, the curves are affine between 400 and 500°C. However, the curves obtained at 300°C and below do not belong to the family of curves obtained at 400–500°C. This probably

indicates that the reaction zone has a complex structure or the reaction mechanism changes as the temperature decreases to 300°C. However, for Co/Q-3, the conversion-vs.-time curves are affine within the experimental error throughout the temperature range examined.

The possibility of internal diffusion control should be taken into account in the analysis of the reduction kinetics of metal oxides on porous supports. The fact of internal diffusion control can be established by varying the granule size. For Co/Q-3, the reduction rate does depend on the support granule size, indicating that the reaction is controlled by internal diffusion.

The internal diffusion control is also indicated by the dependence of the reduction rate on the average pore size of the support in the systems examined. Mass transfer in narrow pores during reduction results in a local increase in the partial pressure of water vapor, and, as a consequence, the chemical equilibrium shifts towards the oxide. In turn, CoO interacts readily with the silanol groups of the silica gel to produce cobalt silicate, which is difficult to reduce. The encapsulation of Co nanoparticles in narrow pores is also possible. In this case, the reduced metal particles are "locked" in the support pores and are incapable of adsorbing gas. The existence of such particles is indicated by the fact that neither O_2 nor CO is adsorbed on Co/Q-3, while considerable magnetization persists. Similar results were obtained in [24]: superparamagnetic Co particles 5 nm in size are not oxidized on contact with air. It is believed that this is due to the encapsulation of the Co particles in the narrow silica gel pores [24].

Effect of Preparation Conditions on the Cobalt Particle Size and the Shape of the Particle Size Distribution Function

As mentioned above, the parameters of each stage of catalyst preparation affect the parameters of the Co particle size distribution. Let us consider the regularities that have been established by the magnetic particle size analysis of Co/support catalysts prepared under varied conditions.

Drying time and temperature. Water evaporation from a porous support at the drying stage is controlled by capillary forces. Therefore, the rate of water removal is determined by the pore structure of the support. In the general case, the smaller the average diameter of the support pores, the lower the rate of water removal. The ultimate result of slow evaporation is that the solute concentration in fine pores grows in going to the center of the porous particle. However, rapid evaporation results in solute deposition on the external grain surface. Thus, the drying rate can depend on the flow rate of the drying gas. The studies dealing with catalyst preparation have ignored this fact.

The influence of the drying time and temperature on the TPR spectrum was studied for catalysts obtained by impregnating silica gel with a solution of cobalt nitrate

[10]. Lengthening the drying time increases the hydrogen adsorption rate in the temperature range 300–600°C. A similar result is obtained by increasing the drying temperature from 100 to 150°C. It is believed [10] that drying causes the partial decomposition of cobalt aqua complexes, which form hydrogen bonds with silanol groups of the silica gel surface. This hydrogen bonding results in surface cobalt silicates, which are reducible to metal only at high temperatures. Thus, an increase in the drying time and temperature must decrease the probability of surface silicate formation. However, the influence of drying conditions on the cobalt particle size has not been considered [10]. We have demonstrated that lengthening the drying time while maintaining the other parameters at constant values substantially decreases both the Co particle size and the extent of reduction.

Calcination conditions. The influence of calcination conditions on the Co particle size has been insufficiently studied because very complicated topochemical processes occur during cobalt nitrate decompsoition followed by the formation of oxide particles and by the reaction between the oxide and the support.

An increase in the calcination temperature is known to increase the role of the oxide–oxide interaction [25]. For silica gel and alumina, the oxide–oxide interaction produces silicates and aluminates, respectively. The calcination time has a similar effect. The size of cobalt hydroxo complex particles in silica gel pores is 2–2.5 nm. Calcination decomposes these hydroxo complexes, and the resulting oxide aggregates into comparatively large Co_3O_4 particles [26]. The ultimate size of these Co_3O_4 particles is determined by the pore size in the silica gel. Calcination is also accompanied by the partial conversion of Co_3O_4 into CoO above 350°C [27]. CoO reacts with SiO_2 to form Co_3SiO_4. The high concentration of NO_x in the support pores during nitrate decomposition results in the formation of large Co_3O_4 particles. On the contrary, a decrease in the NO_x concentration favors the formation of surface silicates [28]. The NO_x concentration in the zone of cobalt nitrate decomposition during calcination can be controlled by varying the air flow through the catalyst. We have shown that an increase in the air flow rate considerably decreases the Co particle size and extent of reduction, as would be expected. The weight fractions of 0- to 10-nm and 10- to 20-nm particles as a function of the air flow rate for the 10 wt % Co/Q-6 catalyst after reduction at 500°C for 1 h in an H_2 flow (50 cm^3/min) are shown in Fig. 6. The fraction of Co particles smaller than 10 nm increases and the fraction of 10- to 20-nm particles decreases as the air flow rate in calcination is increased.

The calcination temperature exerts a less pronounced effect on the Co particle size distribution. The extent of reduction and the fraction of particles of size 0–10 nm versus calcination temperature are presented in Fig. 7. The extent of reduction as a function of T_{calc}
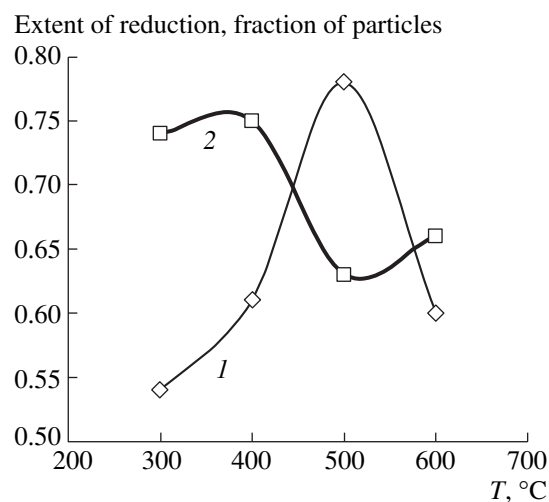
Weight fraction of particles
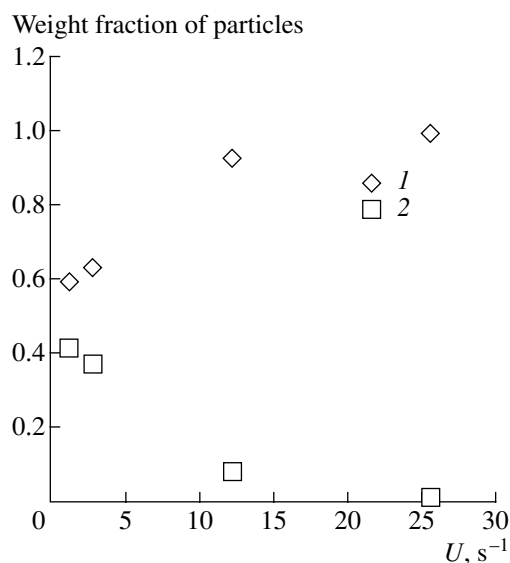
Fig. 6. Weight fraction of particles of size (*1*) 0–10 and (*2*) 10–20 nm versus the volumetric flow rate of air during calcination (*U*) for the 10 wt % Co/Q-6 catalyst that has been reduced in H_2 at 500°C.

Extent of reduction, fraction of particles

Fig. 7. (*1*) Extent of reduction and (*2*) the fraction of particles of size 0–10 nm versus calcination temperature.

has a maximum. The lowest extent of reduction is observed for the particles of size 0–10 nm (that is, rather fine Co particles) at $T_{calc} = 500$°C. The fraction of particles smaller than 10 nm increases with decreasing calcination temperature.

Reduction conditions. As is shown above, the partial hydrogen pressure during reduction determines the average Co particle size. Our studies show that the partial hydrogen pressure exerts a substantial effect on the shape of the Co particle size distribution function. Figure 8 shows experimental distribution functions for the 10 wt % Co/C-80 catalyst (C-80 is silica gel with a specific surface area of 80 m²/g and a pore diameter of 50 nm) reduced at 500°C under two different partial hydrogen pressures. In one case, we used pure hydrogen at atmospheric pressure; in the other, a mixture of 5 vol % H_2 and Ar. In both cases, a bimodal size distribution of Co particles is observed. The volume fraction of the particles of size 5–9 nm is larger for pure hydrogen. By contrast, the particles of size 9–14 nm prevail in the case of a reduced partial pressure of H_2 (H_2 + Ar). This suggests, in particular, that the dilution of hydrogen with nitrogen, which is frequently used in catalyst preparation, can increase the average particle size.

The metal particle size depends on the hydrogen flow rate, because it depends on the local concentration of water vapor evolved during reduction. Figure 9 presents experimental distribution functions for the Co particles obtained after the 10 wt % Co/C-80 catalyst was reduced in pure hydrogen and in hydrogen saturated with water vapor at room temperature.

It is noted in some publications that proceeding to the reduction step without performing calcination

decreases the average particle size [24]. However, this method of catalyst preparation demands much more hydrogen and is, therefore, impracticable.

The particle size distribution depends strongly on the rate at which the sample was heated to the reduction temperature. The fraction of large particles increases at high heating rates. At a given temperature, lengthening the reduction time coarsens the Co particles [29]. As for the reduction temperature, the influence of this factor on the size distribution of Co particles remains unclear. However, we believe that increasing the reduction temperature will favor two opposite processes. On the one hand, an increase in reduction temperature will result in

Volume fraction of particles
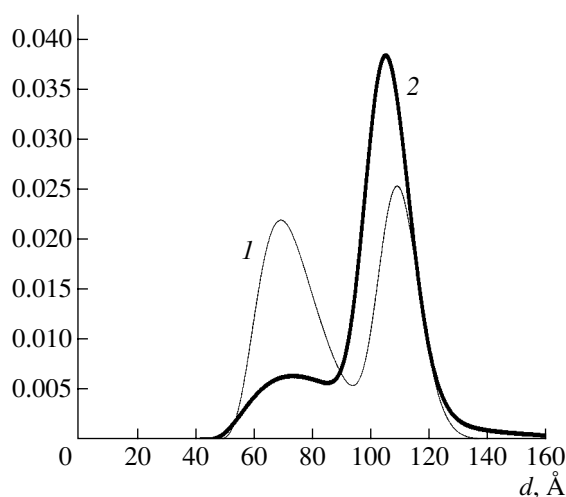
Fig. 8. Size distribution functions for Co particles in the 10 wt % Co/C-80 catalyst reduced at 500°C and different partial hydrogen pressures: (*1*) 1 atm H_2 and (*2*) 5 vol % H_2 + Ar mixture.

Volume fraction of particles
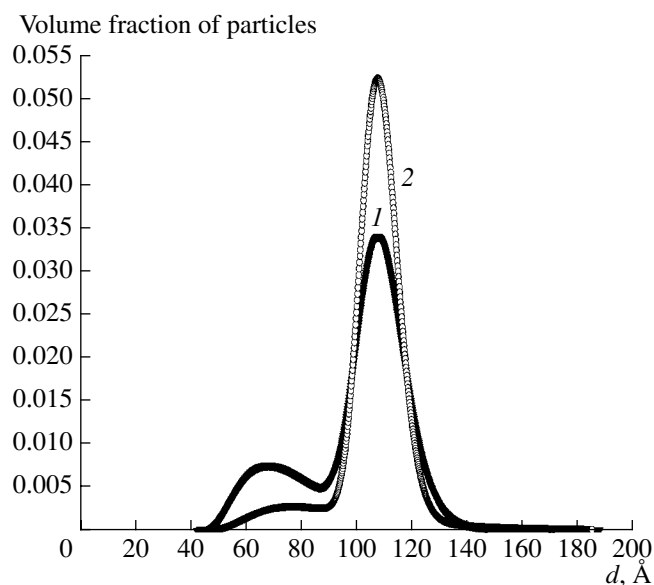
Fig. 9. Size distribution functions for the Co particles obtained after the 10 wt % Co/C-80 catalyst was reduced at 300°C in (*1*) pure hydrogen and (*2*) hydrogen saturated with water vapor at room temperature.

particle sintering and, correspondingly, coarsening. On the other hand, an increase in the reduction temperature will lead to the reduction of the fine oxide particles localized in narrow support pores and, as a consequence, the proportion of fine particles will increase.

ACKNOWLEDGMENTS

REFERENCES

1. Iglesia, E., Soled, S.L., and Fiato, R.A., *J. Catal.*, 1992, vol. 137, p. 212.
2. Fu, L. and Bartholomew, L.C.H., *J. Catal.*, 1985, vol. 92, p. 376.
3. Reuel, R.C. and Bartholomew, L.C.H., *J. Catal.*, 1984, vol. 85, p. 78.
4. Ishihara, T., Egichi, K., and Arai, H., *J. Mol. Catal.*, 1992, vol. 72, p. 253.
5. Chin, R.L. and Hercules, D.M., *J. Phys. Chem.*, 1982, vol. 86, p. 360.
6. Kraum, M. and Baerns, M., *Appl. Catal.*, 1999, vol. 186, p. 189.
7. Riva, R., Miessner, H., Vitali, R., and Del Piero, G., *Appl. Catal.*, 2000, vol. 195, p. 111.
8. Rosynek, M.P. and Polansky, C.A., *Appl. Catal.*, 1991, vol. 73, p. 97.
9. Sun, S., Tsubaki, N., and Fujimoto, K., *Appl. Catal.*, 2000, vol. 202, p. 121.
10. Van Steen, E., Sewell, G.S., Makhothe, R.A., *et al.*, *J. Catal.*, 1996, vol. 162, p. 220.
11. Chernavskii, P.A., *Zh. Ross. Khim. O–va im. D. I. Mendeleeva*, 2002, vol. 46, p. 19.
12. Petrov, Yu.I., *Fizika malykh chastits* (Physics of Small Particles), Moscow: Nauka, 1982.
13. Weil, L., *J. Chem. Phys.*, 1954, vol. 51, p. 715.
14. Sudarikova, N., Perov, N., Bagrets, A., Lermontov, A.S., Pankina, G.V., and Chernavskii, P.A., *J. Magn. Magn. Mater.*, 2004, vols. 272–276, p. 1565.
15. Chernavskii, P.A., Lermontov, A.S., Pankina, G.V., Torbin, S.N., and Lunin, V.V., *Kinet. Katal.*, 2002, vol. 43, no. 2, p. 292.
16. Chernavskii, P.A., *Zh. Fiz. Khim.*, 2003, vol. 77, p. 636.
17. Morel, R., Brenac, A., and Portemot, C., *J. Appl. Phys.*, 2004, vol. 7, p. 3757.
18. Chernavskii, P.A., Pankina, G.V., Lermontov, A.S., and Lunin, V.V., *Kinet. Katal.*, 2003, vol. 44, no. 5, p. 718.
19. Morokhov, I.D., Petinov, V.I., *et al.*, *Usp. Fiz. Nauk*, 1981, vol. 133, p. 653.
20. Poltorak, O.M. and Chukhrai, E.S., *Fiziko-khimicheskie osnovy fermentativnogo kataliza* (Physicochemical Foundations of Enzyme Catalysis), Moscow: Vysshaya Shkola, 1971.
21. Chernavskii, P.A., *Zh. Fiz. Khim.*, 2004, vol. 78, p. 1.
22. Huijuan Bi, Weiping Cai, and Caixia Kan, *J. Appl. Phys.*, 2002, vol. 92, p. 7491.
23. Barret, P., *Cinétique hétérogéne*, Paris: Gauthier Villars, 1973.
24. Barbier, A., Tuel, A., Arcon, I., Kodre, A., and Martin, G.A., *J. Catal.*, 2001, vol. 200, p. 106.
25. Chernavskii, P.A. and Lunin, V.V., *Kinet. Katal.*, 1993, vol. 34, p. 531.
26. Castner, D.G., Watson, P.R., and Chan, I.Y., *J. Phys. Chem.*, 1989, vol. 93, p. 3188.
27. Khodakov, A.Yu., Griboval-Constant, A., and Bechara, R., *J. Catal.*, 2002, vol. 206, p. 230.
28. Coutler, K.E. and Sault, A.G., *J. Catal.*, 1995, vol. 154, p. 56.
29. Lermontov, A.S., *Cand. Sci. (Chem.) Dissertation*, Moscow: Moscow State Univ., 2003.